THE PENROSE, AMMANN, AND DA TILING SPACES ARE CANTOR SET FIBER BUNDLES

R. F. WILLIAMS

Dedicated to Jacob Palis at 60 and Steve Smale at 70

ABSTRACT. Anderson and Putnam [AP] have recently shown that the space of all tilings of a substitution tiling scheme is a special case of the present authors "expanding attractor" [W2]. This resurrects an earlier conjecture [W2] of the present authors, in this special case.

Conjecture 0.1. *The tiling space of a substitution tiling space is a fiber bundle over the torus, with Cantor set fiber.*

If true, this could be important in the classification of these spaces, just as in the 1-dimensional case, [BLV]. These spaces were known (in these 2 disciplines) to be locally the product of a disk and a Cantor set. Farrell and Jones [FJ] gave an example showing our more inclusive conjecture is false. Here we show that the Penrose, Ammann and "stepped plane", tiling spaces are in fact such bundles. Among dynamicists, the stepped plane tiling space (in special cases), is known as the "DA"attractor of Smale. The formalism of substitution systems provides a Markov partition, and this is certainly part of their intuitive appeal. However, in dynamics such partitions are rare in dimensions > 2 and do not occur for the DA attractor. We consider below a weaker concept, that omits this requirement. Finally, we construct an example like the Farrell-Jones example, in sufficient detail that it can be visualized as a *smooth tiling space*, as opposed to the more rigid *geometric tiling space*.

Mathematics subject classification(1985 revision). Primary 58F13, 54F15. Key words: tiling, expanding attractor, branched surface generalized solenoid, Cantor fiber bundle.

This is the first paper I have written which contained the word, tiling. As this paper is being circulated while in progress, the figures are labeled by a phrase referring to their contents. All corrections and suggestions are solicited. special thanks are due to Chaim Goodman-Strauss and Ian Putnam; John Leucke, Nic Ormes, and Charles Radin have also been helpful.

1. Introduction

The basic building block here is the branched manifold, introduced to study hyperbolic attractors. In [W2] there is a detailed foundation of these; the dimension 1 case [W1] is applied extensively by the group around Thurston (and called "train-tracks.") We include here enough of the definitions for most readers to understand the 2 dimensional case. A smooth branched surface is a metric space in which each point has a neighborhood like an open set in the smooth space indicated in figure Ramified Branch Point. These various neighborhoods are held together by transition maps just as in the definition of a manifold. As mentioned below, figure Ramified Branch Point is *not* the generic case. In fact, the branched manifold occurring in the construction of Anderson-Putnam are usually quite far from generic. Thus we need the more general formulation as given in [W2]. In particular, in the Penrose case, some points have neighborhoods which are the union of no fewer than 10 smooth disks, (see below). By a *hyperbolic attractor* for a diffeomorphism f is meant a compact set which is mapped into a neighborhood of itself by f, and has a hyperbolic structure (see Smale, [S] or [R, p241]). An *expanding attractor* or *generalized solenoid* is a hyperbolic attractor whose topological dimension is the dimension of its expanding direction. For a map $f : X \to X$, the *universal extension* of f is the map $\hat{f} : \hat{X} \to \hat{X}$, where $\hat{X}$ is the set of all sequences $x = (x_0, x_1, x_2, ...)$ such that $f(x_i) = x_{i-1}, i = 1, 2, ...$ and $\hat{f}(x)_i = x_{i+1}$. Then the *shift map* $\hat{f} : \hat{X} \to \hat{X}$, just drops the first coordinate of a point and is a homeomorphism. Finally, in [W2] we characterized expanding attractors of dimension n as being topologically conjugate to the natural extension $\hat{g} : \hat{K} \to \hat{K}$ of an immersion $g : K \to K$, where K is an n dimensional branched manifold and g is an immersion such that

1. The map g has a dense orbit.
2. for each $x \in K$ there is a neighborhood N of x and an integer j such that $g^j(N)$ is a subset of a smooth n-cell. [Hence by compactness of K, such a j can be chosen for all x.]
3. g is an expanding map.

In the striking paper of Anderson-Putnam [AP], they show that the dynamics of the inflation or substitution tiling requires precisely these 3 ingredients. Note, as a partial converse, that beginning with an expanding attractor, a smooth but perhaps not geometric tiling is induced on each unstable plane $W^u(x), x \in \hat{K}$ as follows

1. Each unstable plane $W^u(x), x \in \hat{K}$ maps by the projection $p : \hat{K} \to K$ of the attractor onto its one of its coordinates, K. Note that $p|W^u(x)$ is an immersion.
2. The branch lines of K separate K into *cells* $\{C_i\}$ and the pull backs of the cells to the plane $W^u(x)$ forms a tiling of the plane.
3. As there are only finitely many cells in K, it follows that there are only finitely many types of tiles.
4. The unstable planes are as smooth as the inducing map, but there is no reason for them to be flat.

The 1-dimensional case of this characterization, gives us an effective way of construction examples. But in higher dimensions, few examples were known; we had the "DA" maps of Smale [S] and the ingenious but difficult construction of Farrell-Jones [FJ].

From this point of view, tilings give us a rich new source, though again, the construction of tilings seems to be more an art than a science. The authors of [BJV] also discuss the following result, mostly in the 1-dimensional case.

Remark 1.1. *The space of all unstable manifolds $\{W^u(x), x \in \hat{K}\}$, with the tiling given above is a smooth "substitution" tiling space.*

Proof Essentially the only geometric content of this remark is the analog of of the substitution rule. For this, note that the expanding map $g : K \to K$, of one coordinate space into the previous, induces a subdivision of the cells of the first coordinate space. Further, that these subdivided pieces are mapped into the second coordinate space, where they form a partition of the cells there. Hence, they can be amalgamated to the original cells. Then as the following diagram is commutative,

$$\begin{array}{ccc} W^u(x) & \xrightarrow{\hat{g}} & W^u(y) \\ {\scriptstyle q}\downarrow & & \downarrow{\scriptstyle q} \\ K & \xleftarrow{g} & K \end{array}$$

we see that the tiling of $W^u(x)$ is subdivided, sent to the tiling of $W^u(y)$, where it amalgamates into that tiling. See the illustration at the bottom of http://www.ma.utexas.edu/page/dynsys.html

2. Questions and conjectures

Conjecture 2.1. *Every substitution tiling space is the total space of a fiber bundle over a torus with Cantor set fiber.*

Here we do not need Markov partitions. As mentioned in the abstract, Markov partitions are implicit in the usual formalism of substitution tilings. One way of formulating this assumptions in our setting, is to assume that the map

$$\hat{g} : \hat{K} \to \hat{K}$$

has a Markov partition of the form $E \times C$, in which E is a tile and C is a cantor set. On the branched surface K this means that for each tile $E, g(E)$ is a union of tiles. We believe

Conjecture 2.2. *If K is a branched surface containing a 2-sphere, then there is no immersion g of K into itself satisfying axions 1,2,3+ for which the image of each tile is the union of a set of cells.*

However, by Rufus Bowen's Theorem, [R, 283f] Markov partitions do always exist though the cells will mostly be fractal, see Thurston [T]. Since unstable manifold *are* planes, our example below does yield a *smooth* tiling of the usual (flat) plane. By this we mean that there is a partition of the flat plane into cells each of which is diffeomorphic to one of our finite set of prototiles. For a Farrell-Jones type of example, there certainly is distortion of some tiles. We believe

Conjecture 2.3. *For the example below, or for any example in which K contains a smooth sphere, there is infinite distortion. I.e., there is a tile for which the various copying diffeomorphisms have unbounded first derivative.*

Conjecture 2.4. *By the internal symmetry, the fiber bundle of Penrose tiling space can be given in 5 ways; we conjecture that there are no more, up to homotopy. See below.*

3. Tiling spaces as Cantor bundles

The branched surfaces K with $\hat{K}$ a geometric tiling space are generally speaking rather complicated. However there is one case which is rather simple. This is well known in dynamical systems as the "DA" attractor, and in tiling circles, as a "stepped plane" tiling.

In both guises, these occur in all dimensions. The DA versions correspond to Anosov automorphisms of a torus, and thus more restricted than stepped planes. Stepped plane tilings in general given as "projection tilings." In dimension 1, [MPP] show that they are substitution tilings only in a special case; though I have not had time to digest their paper, this must be precisely when they are the DA attractors associated with a 2×2 Anosov matrix. In dimension 2 the corresponding analysis is carried out, though in other language, in [W4]. Thus the only DA's which are substitution tiling spaces are those corresponding to a real algebraic integer with 2 complex conjugates. Furthermore, the substitution pieces have to be amalgamated to give a finer tiling—and then, it will be rotated. Were there 2 complex conjugates, they would be of different magnitude and distort the tiles. If such distortion is allowed then we have again an identification of DA's and stepped plane tilings.

We begin this section with a description of this example in dimension 2 and show that $\hat{K}$ *is* a fiber bundle over the torus. The proof given applies, with obvious changes, in all dimensions.

Theorem 3.1. *The tiling space of the stepped plane is a Cantor set fiber bundle.*

Proof Though the simplest of the tilings, the DA has deep connections with arithmetic and continued fractions. We have studied these attractors in [W3,4], but will include enough here for most readers; the construction will be given in dimension 3 for simplicity.

We describe K in terms of the projection of 3 adjacent faces of the standard cube onto a plane. In detail, let Π be a plane and v a vector in $\mathbb{R}^3$, where both v and the normal to Π have all positive coordinates. Let $q : \mathbb{R}^3 \to \Pi$ be the projection parallel to v. Then the basis vectors project to 3 directions, $\{v_i\}$ having the origin as a convex combination. The faces of the cube project to 3 parallelograms P_j with sides parallel to the v_i, taken 2 at a time. The P_j are the cells of the branched surface $K = P_1 \cup P_2 \cup P_3$, with the opposite sides of each of the parallelograms identified by a translation (see figure DA). Thus K is the union of 3 tori, each 2 meeting along a circle, and up to homotopy, K is the 2 skeleton of the 3 dimensional torus.

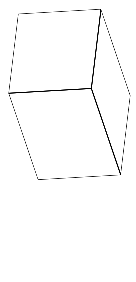

Figure DA

Let $Q = P_1 \cup P_2 \cup P_3$, be the disk before identifying the edges.

Choose 3 vectors in $\mathbb{Z}^2$, such as $(1,0),(0,1),(-1,-1)$, having the origin as a convex combination, and spanning 3 parallelograms each having area 1. Then define the map $f : K \to \mathbb{R}^2$ to send the v_i to the chosen vectors, and the cells of K into the corresponding parallelograms. This map composed with the quotient $p : \mathbb{R}^2 \to \mathbb{R}^2/\mathbb{Z}^2 = T^2$ is a topological immersion, though the derivatives are not continuous along the intersections of the cells. That is to say, there is no folding because the identifications are by translations in both cases.

Finally, the map $p \circ f \circ \pi_0 : \hat{K} \to T^2$, is a fiber bundle, where π_0 is the projection of $\hat{K}$ onto its first coordinate. (See the definition of the *universal extension*, $\hat{X}$ in the Introduction.) The particular universal extension, $\hat{K}$, is the tiling space itself and is a fiber bundle over the torus, with Cantor set fiber. Thus giving the 2 automorphisms corresponding to 2 generating circles of the base, would be an effective way to describe it, both as bundle and topological space. This is beyond the scope of this paper. We illustrate the stepped plane with the DA of the linear map of the 3-dimensional torus induced by the following matrix:

$$\begin{pmatrix} 0 & 1 & 0 \\ 0 & 0 & 1 \\ 1 & 0 & 1 \end{pmatrix}.$$

See figure Stepped Plane.

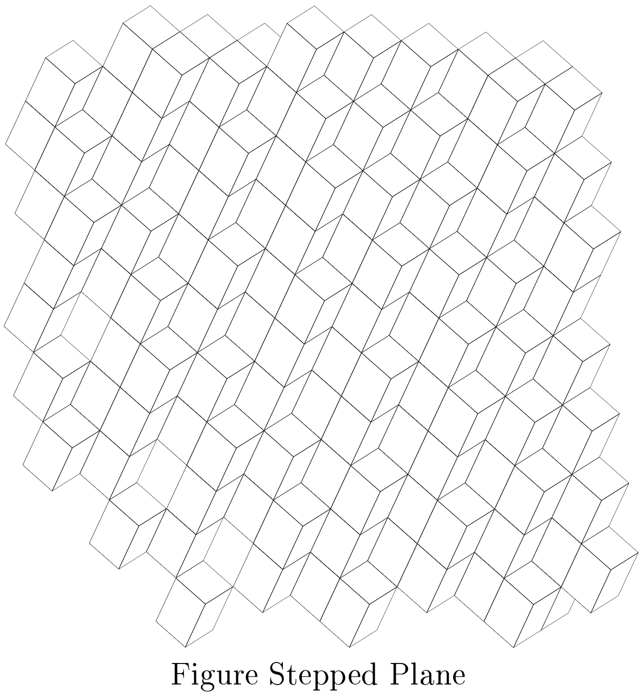

Figure Stepped Plane

Note that up to now we have not used our special assumptions so that our proof applies to stepped plane tiling spaces quite generally. (We leave aside here tilings of the line.) There are three levels: the DA attractor happens for any codimension 1 Anosov diffeomorphism, it is the stepped plane example for linear Anosov diffeomorphisms of a torus in some dimension, and is a substitution and amalgamation system only for the 3 dimensional torus, where the linear map has one real and 2 complex eigen values. Finally, we define here the substitution rule, in the last case. The vector v is an eigen vector corresponding to $\lambda > 1$, and the plane Π the plane of the other 2 eigen vectors, assumed < 1 in norm, of a linear map, say A of the torus, $\mathbb{T}^3$. Then the "DA" is defined as the composition $F = \phi \circ A^{-1}$ where ϕ is

1. the identity outside a small neighborhood of the origin, and
2. near the origin, a strong push away from the plane Π, in such manner as to leave the lines parallel to v invariant.

Then F has the origin as a repellor and an expanding attractor Λ; then, using standard tricks,(see [W4] for example), we can take K and Q as above. If necessary, we raise F to a power n so that $F^n(Q) \supset Q$. Using the tricks introduced in an earlier paper, [W3], we can use the original linear map to make pictures. These make use of the projection onto the eigen plane Π, of the complex eigenvalues and the natural inner product on Π.. In this inner product, the invariant ellipses associated with the complex eigen values, are circles.

The graphics of the stepped plane tiling, or equivalently, an unstable plane in the DA of a 3 dimensional Anosov matrix A, is made as follows; we use the notation $v, v_i, \Pi, P_j, Q, K, A$ from the proof. Here P_1 has vertices which are the projection of the lattice points $O, v_1, v_1 + v_2$, and v_2. The other P's are determined similarly. We have arranged for K to be the base of a fundamental domain D of the 3 dimensional torus in $\mathbb{R}^3$. In turn the domain D is the union of three cylinders, one over each of the P_i. For example, the cylinder over P_1 is the union of all line intervals parallel to v, having one end point on P_1 and the other end point on the plane $\Pi + v_1 + v_2$, (that is, the translation of the plane Π by the vector $v_1 + v_2$.)

The unstable plane about O is determined by taking a small disk in Π around the origin, then applying repeatedly some map, A^{-1} in this case. This yields a bigger and bigger subdisk Δ, of our unstable plane in Π. Thus our tiling is obtained by intersecting Δ with all of the *other* fundamental domains which also intersect the plane Π. Since some of these fundamental domains are "in front" of others, they are printed later so as to obscure the disks "in back", which are printed earlier in our computer program. Since we consider only finitely many of the fundamental domains, errors in our graphics are introduced near the boundary of the disk Δ. The reader can easily spot these errors in the figure Stepped Plane.

Another problem with this way of getting a graph, is that we cannot make a ©PostScript file to print 2 of these together. This prevents us from including a full graph of a stepped plane with one of its "subdivisions." We can print the second on the same paper the first was printed on, or use the copying machine this way. See our home page.

Theorem 3.2. *The Penrose tiling space is a fiber bundle over the torus with fiber the Cantor set.*

Proof We use the version of the Penrose tiling given in Anderson-Putnam [AP] sticking to their notation [AP figure 6, p. 535] as well. (See figure Penrose.) Let us denote the 4 pieces on the left side of figure 6, by I, II, III, and $IIII$ from top to bottom. (We have corrected a typo in figure 6 of [AP]; the two sides labeled 27 are labeled 22 in our figure II. typo in figure 6: the 2 sides labeled 27 in II should actually be 22.)

We feel that the reader will be aided by a few preliminary remarks:

Remark 3.3. *Two smoothness structures occur here: their flat structure as a tiling, and their structure as a smooth branched manifold.*

Remark 3.4. *Pieces I and II are topological surfaces of genus 2. However both the flat structures given have 2 (and only 2) vertices with excessive angles; these have angles 4π and are the points $\{\beta, \gamma\}$ in I and $\{\alpha, \delta\}$ in II.*

Proof In I the 10 triangles have angle totals of 10π, with α getting only 2π. Thus β and γ get 4π each. Similarly for part II.

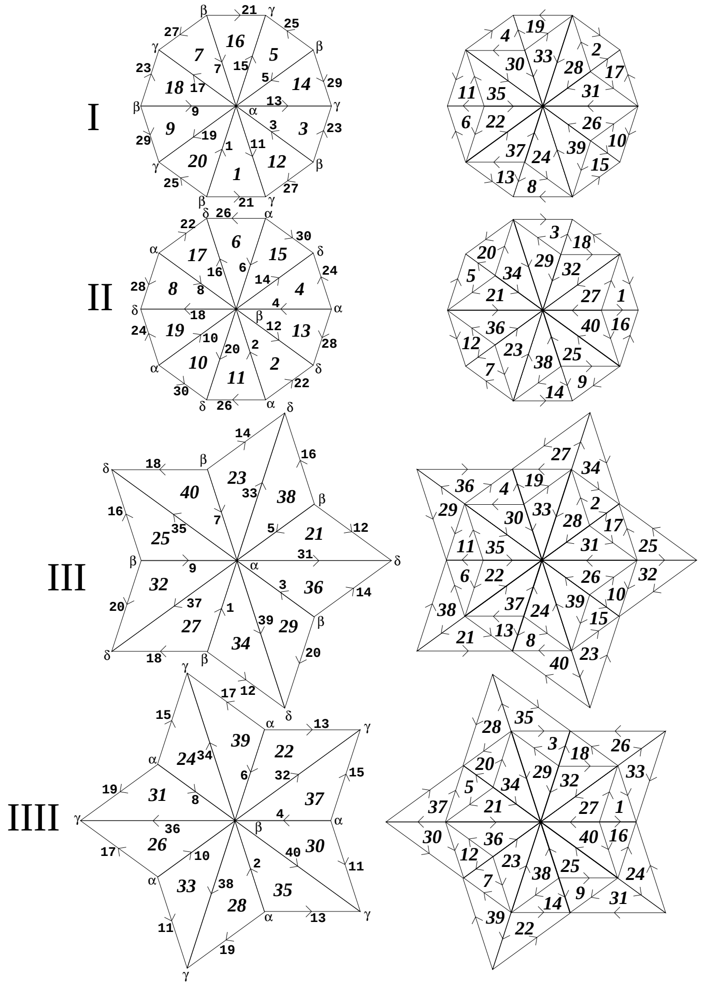

Figure Penrose

Remark 3.5. *Pieces III and IIII are topological surfaces of genus 1 but there is a single point of excess angle* 6π *according to the flat structure. This is* β *in III and* α *in IIII.*

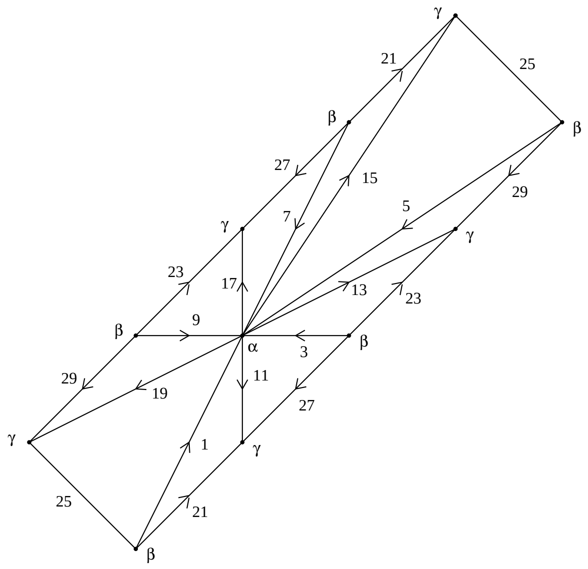

Figure I

Remark 3.6. *In particular, these pieces are not branched surfaces as the bad points do not have a neighborhood that is the union of smooth disks. However, the whole* $K = I \cup II \cup III \cup IIII$ *is a smooth branched surface using the flat structure as a smooth structure.*

Proof This property is required of a branched surface, (see [W2, p.172]) and fortunately, it is implicit in the "boundary forcing property" of substitution tiling spaces. To see this directly: part I of figure Penrose splits into 5 "kite shaped" disks and these together form a neighborhood of β. The other 3 II, III, and IIII split into into 5 regions forming the neighborhoods of α, δ and γ respectively. (IIII because the high level graphing program turns my IV upside down.)

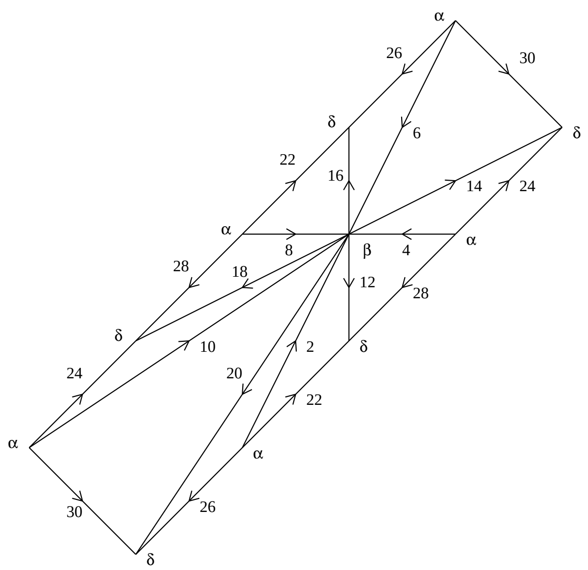

Figure II

From the first remark above we see that an immersion of I into the torus will be of degree 2 near the 2 special points of I, (like $z \to z^2$ in complex variables). This has consequences for the degree of any immersion of I. The simplest possibility is that β is the only point of I having the same image as β. Assuming this and the corresponding thing for δ, the degree must be 2 on the rest of I as it is connected. Thus we should first try an immersion of degree 2—and happily this works. Similarly, the degree for II will be 2, and our immersion will have degree 3 on III and $IIII$.

We proceed by giving an immersion of each of the *figures* I, II, III, and $IIII$, into the plane so that composed with the quotient map, $\mathbb{R}^2 \to \mathbb{R}^2/\mathbb{Z}^2$, the resulting map will agree on the various parts of our figures which are to be identified. The maps given in figures I, II, III, and IIII are in fact affine on each triangular disk, so that this agreement is the only additional fact that we have to check. First note that β is always a lattice point, α is a point of the form $(i+1/2, j)$, γ of the form

$(k+1/2, l+1/2)$, and δ of the form $(m, n+1/2)$, where $i, j, k, l, m, n \in \mathbb{Z}$.

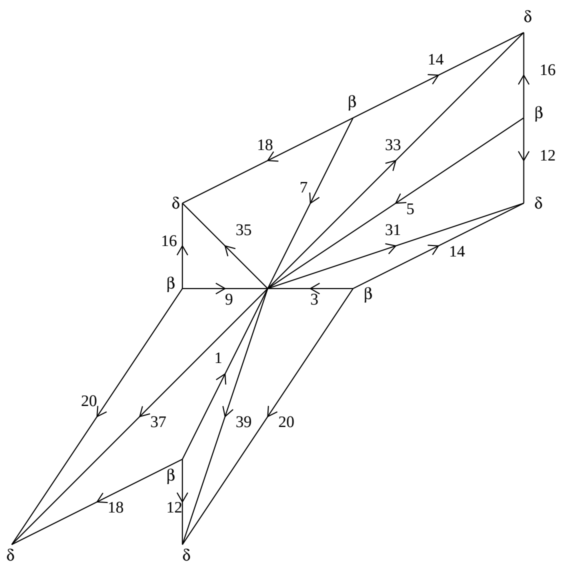

Figure III

Thus we need only look further for the agreement on the edges; now $I \cap II = \emptyset, I \cap III = \{1, 3, 5, 7, 9\}$, where these last mean the edges so numbered. But these are embedded, respectively, as

$$x/2 + y, -x/2, -3x/2 - y, -x - y/2, x/2,$$

in both cases, beginning at a lattice point β. Here x and y are horizontal and vertical unit vectors. Next $I \cap IIII = \{11, 13, 15, 17, 19\}$ and these are embedded as

$$-y/2, x + y/2, 3/2x + y/2, y/2, -x - y/2$$

in both cases beginning at α in both cases. Proceeding, $II \cap III = \{12, 14, 16, 18, 20\}$ where these are embedded as vectors

$$-y/2, x + y/2, y/2, -x - y/2, -x - 3y/2$$

beginning at β in both cases. finally $II \cap IIII = \{2, 4, 6, 8, 10\}$ and these are embedded as vectors

$$x/2 + y, -x/2, -x/2 - y, x/2, 3x/2 + y$$

beginning at α in both cases. This completes the proof of the theorem.

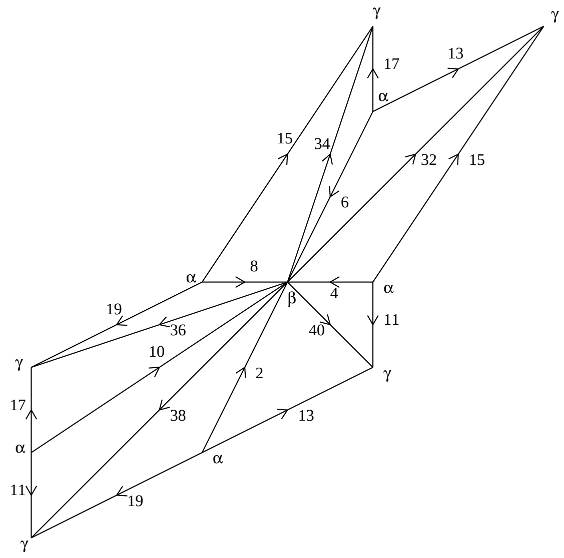

Figure IIII

Theorem 3.7. *The Ammann tiling space is a fiber bundle with Cantor set fiber.*

Proof The following proof is quite general and applies to any tiling by tiles with all edges parallel to one of the the axes. The unit square Q in the plane has 2 horizontal sides, say T, B and 2 vertical sides, say R, L. Let K be the corresponding branched manifold; we proceed to find an immersion of K into the fundamental domain, Q of the torus. By adding vertical sides, if necessary, we may assume that K is a planar figure, with certain segments to be identified with each other. By adding horizontal and vertical sides, is necessary, we may assume that our figure is subdivided into quadrilaterals with 2 roughly horizontal and 2 roughly vertical sides. Then map each of these quadrilaterals into the square Q sending the four edges into Q in the natural way. Composing with the identifications making Q into a torus, we get the required immersion. For example, this construction applied to complex as presented in Anderson-Putnam, [AP, figure 4,p533], yields 8 quadrilaterals for each of the large tiles and 3 for each of the small ones. Thus the immersion is of degree 44.

Remark 3.8. *Since the torus is also obtained from a hexagon by identifying opposite sides, the previous proof can also be applied to tiles spaces with tiles made from hexagons, as in Martin's book, [M,ch 10].*

4. A Farrell-Jones like Example

Farrell-Jones use the machinery described in the introduction, [W2], and thus construct a map $g : K \to K$, in which K is a branched surface and g is an immersion. g is defined by composition in the following diagram,

$$\begin{array}{ccc} K & \xrightarrow{I_n|K} & B_n \\ I\uparrow & & \downarrow\rho_n \\ Y & \xleftarrow{J} & B_1 \end{array}$$

given as their equation 4.1, p.120, in which the spaces are all oriented branched surfaces, the maps are all orientation preserving immersions, B_1 is invariant under the lattice $\mathbb{Z}^3$, J is the quotient map $B_1 \to Y$, and K and Y are compact.

Our construction is a variation. Here we define Y as the quotient of a branched surface $K' \subset \mathbb{R}^3$ which is invariant *only* under the 2-dimensional lattice, $\mathbb{Z}^2$. $\mathbb{R}^2$ with the lattice structure of $\mathbb{Z}^2$ is pictured as the plane of the paper, and lying in $\mathbb{R}^3$. Then K' is a branched surface which is the union of

1. small 2-spheres, $s(z)$ one centered at each vertex $z \in \mathbb{Z}^2$.
2. small tubes, one around each of the edges, which join the 2-spheres in pairs and are tangent to the spheres.
3. smooth disks, or plates, 2 for each square with vertices adjacent points in $\mathbb{Z}^2$, tangent to the previous parts, where they touch.

The spheres of part 1 are smooth but not round, see figure Spheres.

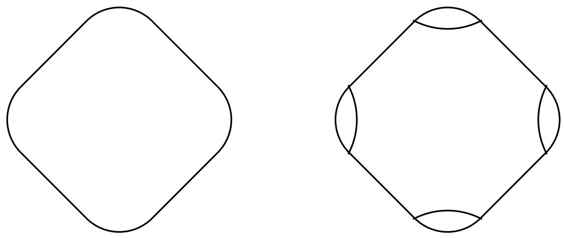

Figure Spheres

At this point we have to give additional structure relating to the individual tiles—which of course did not concern the authors of [EJ]. Each sphere $s(z)$ is composed of two *octagons*,$O(z), O'(z)$, one hidden exactly behind the other, and four round disks, $dr(z), dl(z), dt(z)$, and $db(z)$, on the right, left, top and bottom respectively. See the second part of figure Spheres.

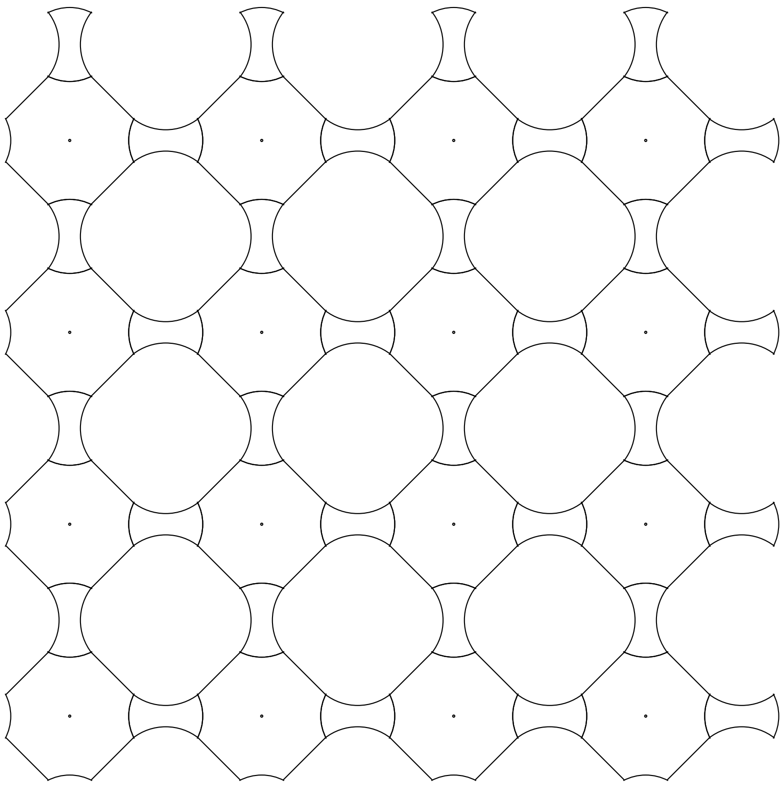

Figure Wallpaper

Next, smooth cylinders, "tubes" in [FJ], are added connecting the spheres; these are of 2 types:

1. *arms* stretching horizontally between adjacent spheres, say $a(x, y)$ attached to $s(x, y)$ at $\partial dr(x, y)$ and to $s(x+1, y)$, at $\partial dl(x+1, y)$.
2. *legs* stretching vertically between adjacent spheres, say $l(x, y)$ attached to $s(x, y)$ at $\partial dt(x, y)$ and to $s(x, y+1)$, at $\partial db(x, y+1)$.

The tangencies are so chosen that the union of the spheres and tubes contains a smooth neighborhood of the cubical 1-skeleton and whose outer boundary is a smooth surface. See figure Wallpaper.

The "arms" $a(z)$ are subdivided into 2 halves, $A(z)$ in the front and $A'(z)$ behind; similarly, the "legs" $l(z)$ are subdivided into a front, $L(z)$ and back half, $L'(z)$. Finally, "plates" $P(z), P'(z)$ are added so that the resulting branched surface is acyclic. In order to keep this structure as simple as possible, the boundary of both plates is chosen along the boundaries of the previously chosen "octagons" and "tubes". In detail, the plate $P(x, y)$ (as well as $P'(x, y)$) has boundary composed, in clockwise order, of the following (See figure Boundary of P.)

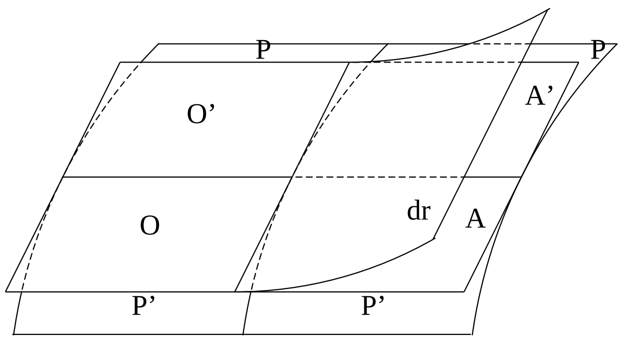

Figure Ramified Branch Point

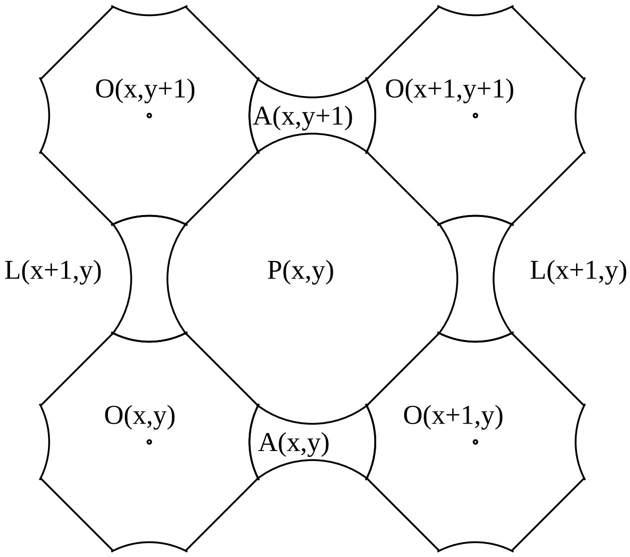

Figure Boundary of P

1. the bottom boundary of $A(x, y + 1)$;
2. the lower left boundary of $O(x + 1, y + 1)$;
3. the left boundary of $L(x + 1, y)$;
4. the upper left boundary of $O(x + 1, y)$;
5. the top boundary of $A(x, y)$;
6. the upper right boundary of $O(x, y)$;
7. the right boundary of $L(x, y)$;
8. the lower right boundary of $O(x + 1, y)$;

In this case, the plate P' is in front of P, since the plate P curves back away from the reader whereas P' curves toward the reader. The tangent planes along their boundaries are perpendicular to the plane of the paper. Thus $P(x, y) \cup P'(x, y)$ is a smooth 2-sphere and both

$$\cup_{z\in\mathbb{Z}^2}(O(z) \cup A(z) \cup L(z) \cup P(z))$$

and

$$\cup_{z\in\mathbb{Z}^2}(O'(z) \cup A'(z) \cup L'(z) \cup P'(z))$$

are smooth planes fairly close to $\mathbb{R}^2$ itself.

All of this structure is chosen to be invariant under the action of $\mathbb{Z}^2$. Y is the quotient space, $K'/\mathbb{Z}^2$, and $q : K' \to Y$ is the quotient map.

In the original work [W2] on branched manifolds, a rather general definition was adopted with a nice, but generic special case *normally branched* delineated as well. Most of the literature on branched surfaces have followed this lead, and only normally branched surfaces are considered. In the present case, our example fails to be normally branched in that (a) along the boundary ∂P of P (and P') our K' is topologically the cross product $I \times X$, of a line interval and an X, instead of $I \times Y$. Also, (b) there are 2 points on each disk where ∂P intersects the boundary of the disk, which are more complicated than the generic case. This is indicated in figure Ramified branch point; the generic case would be as in figure Ramified Branch Point, *without* the plane of P and P'.

5. The map $g : Y \to Y$.

We define the map $g : Y \to Y$, as the composition of a function $g' : Y \to K'$ and the projection q; the composition $g = q \circ g'$ is continuous, though g' is not.

The definition of the map g' : in figure 4 by 4 Sphere, one sees the union of 8 disks, and the front halves of 4 octagons, 2 legs two arms and a plate. Directly behind these are 9 more cells, and their union S is a sphere together with a torus; the sphere and the torus are tangent at their intersection, which is the longitude of the torus and a circle on the sphere. (There are of course, infinitely many copies of S in K', but they all have the same image in Y.) Then g' will immerse the small sphere of Y onto S, with degree 2 on the torus. That is to say, there are orientation preserving immersions of a sphere onto S, of degree n onto the torus, for $n = 0, 1, 2, \ldots$. (That these are the only ones, up to homotopy is also true, but not needed here.) We use one of degree 2 on the torus.

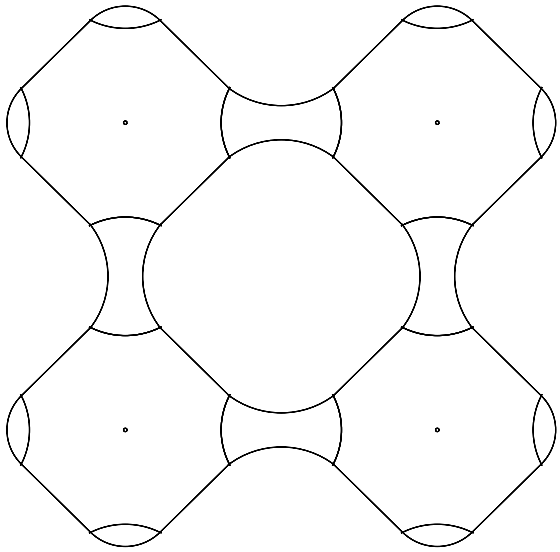

Figure 2 by 2 Sphere

To see the details, we have pictured the cell structure pulled back to the sphere in figure Pull-Back to Sphere. The plate P is in the middle and P' is represented as the exterior of the outer circle. The light dotted lines form part of the boundaries of the 4 disks, (drawn rather crudely, unfortunately; these disks are to be smooth.). Thus, dt is to be mapped (diffeomorphically) onto A and 2 copies of dt, and parts *only* of 2 copies of both O and O'. Similarly for the other 3 disks, summarized in the following:

$$dr \to dr + L'; \quad dl \to dl + L';$$

$$dt \to dt + A; \quad db \to db + A;$$

Next, the heavy dotted lines joining these light dotted lines, together with the 4 disks, separate our picture into 2 pieces, to be the images of O and O'. This is summarized by the equations:

$$O \to P + L + L' + dr + dl; \quad O' \to P' + A + A' + dt + db;$$

Note that wastage here is still just 4 copies of both O and O'. Also, that the expanding axiom is no problem. Finally, since our map comes via an immersion of a sphere, the flattening axiom is automatic so far.

Next we define g' on the arms and legs, beginning with the legs. Note that we have already specified the images of the *end points* of the line intervals, say I, I', separating L and L', since these are also the corner points of O (or O'). In particular, they are the triple points in our partitioning of the branched surface we have called S above. See

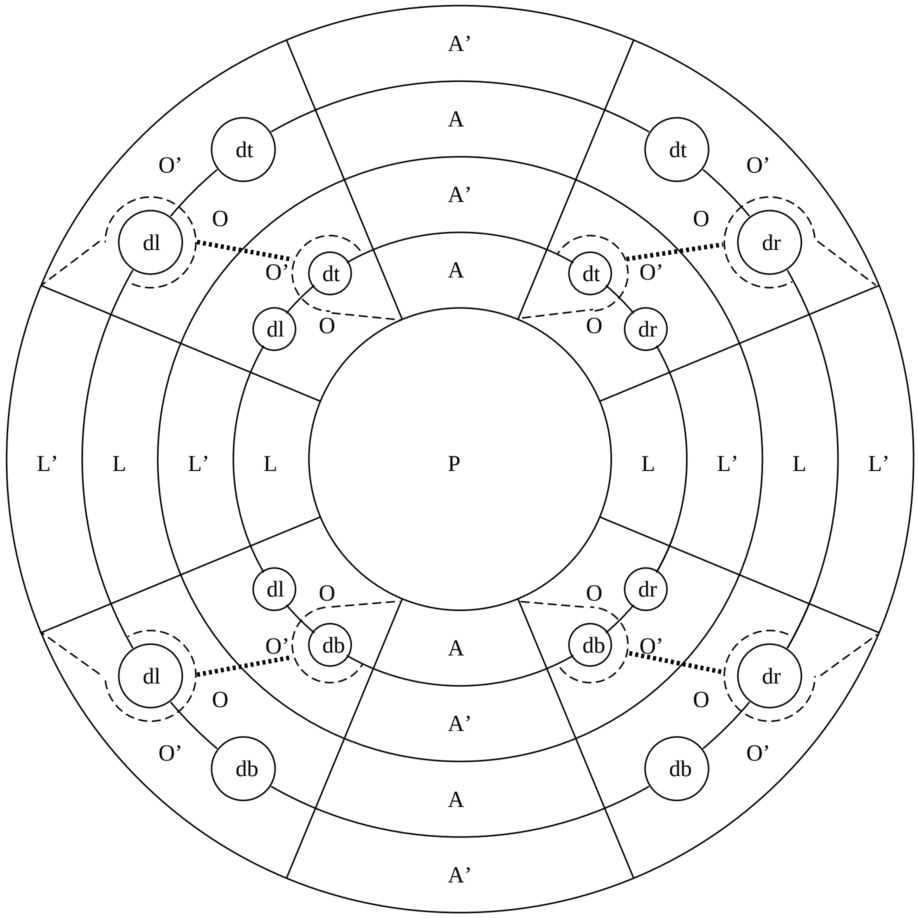

Figure Pull-Back to Sphere

also figure 4 by 4 Sphere, in which are sketched 4 adjacent copies of S, along with these partition lines. Let us refer to them as the NE for north-east, SE, SW and NW copies of S. In figure 4 by 4 Sphere, the images of these triple points together with all $g'(\partial dr)$ in the NW are to the left of the arms joining The NW and NE copies. Similarly, $g'(\partial dl)$ in the NE copy, are to the right of these arms. This means there is room between ∂dr and ∂dl to place *stretched* version of the arm, under g'. Similarly for g' on the leg of Y. Thus we will define $g'(A \cup A')$ to join $g'(\partial dr)$, in NW and $g'(\partial dl)$, in NE. That is to say, the portion of our surface between the simple closed curves,$g'(\partial dr)$, and $g'(\partial dl)$, is an immersed cylinder and the image $g'(A \cup A')$. Similarly, we define $g'(L \cup L')$ to join $g'(\partial db)$, in NE and $g'(\partial dr)$, in SE. Note also that since this last is in the same surface as $g'(S)$, the collapsing axiom holds so

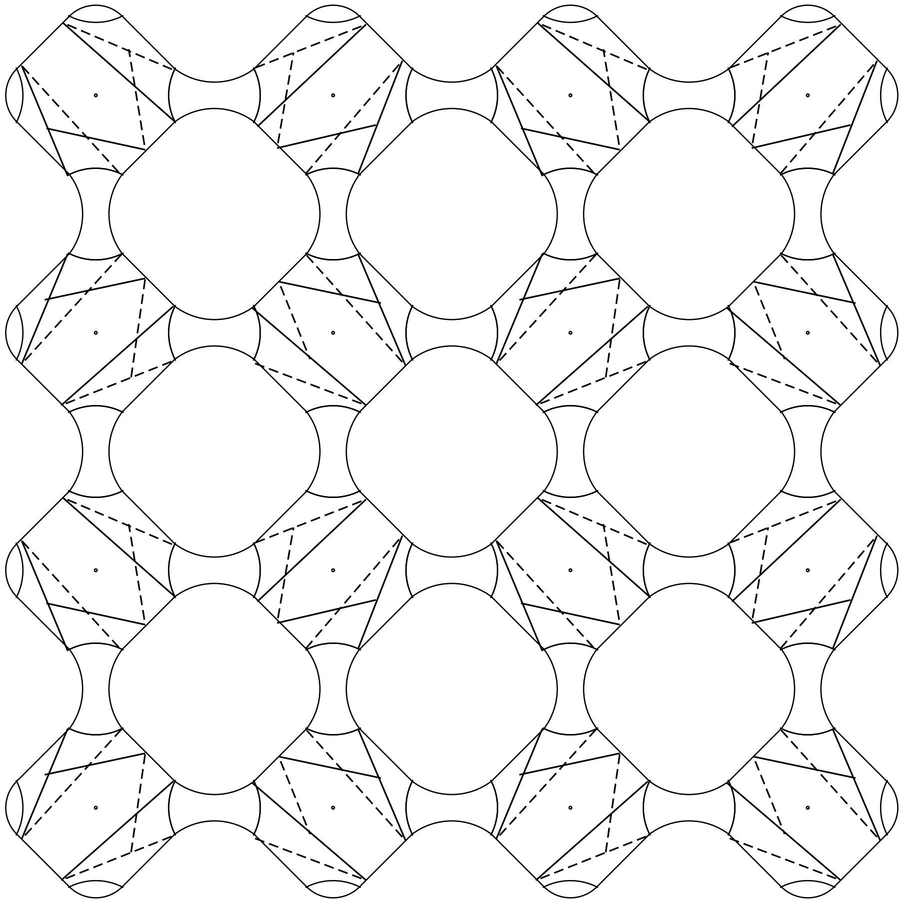

Figure 4 by 4 Sphere

far. Thus we have

$$L \to P + A + L + L'; A \to P;$$

$$L' \to P'; A' \to P' + A + A' + L';$$

At this stage we have mapped various parts of Y onto all 4 of the branches emanating on ∂P, so that we have *not* satisfied the flattening condition yet; this we will do in mapping ∂P, below.

Finally, it remains to define $g'(P)$ and $g'(P')$. In figure 4 by 4 Sphere we see that g' is already defined on $\partial P = \partial P'$. Thus we can consider $g'(\partial P)$ as lying on the copy of S consisting of the middle 4 octagons along with P, 2 copies of A and L, along with the *primes* of these and 2 copies of each of our disks. This is again the image of a sphere immersed onto the central (in figure 4 by 4 Sphere) copy of the branched surface S, and we choose an immersion of degree 2 on the torus, as before.

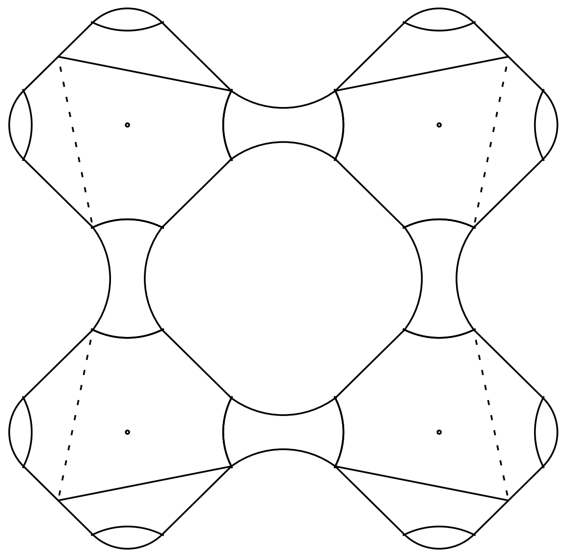

Figure Pull-Back of g'(P')

In figure Pull Back of g'(P') we have sketched the pull back to the sphere under this immersion, just as in the definition of $g'(S)$. In this we see that $g'(\partial P)$, consists of the 4 line intervals in $g'(O \cap O')$, dotted in figure 4 by 4 Sphere, and 4 pieces of the circle at the second level. These last four are the 4 intervals in $g'(A \cap A')$ and $g'(L \cap L')$, and lie mostly in $A \cap A'$, and $L \cap L'$. This simple closed curve (indicated by the dotted lines in figure Pull Back of g'(P')) separates our sphere into 2 disks and we define g' to map P onto the inside one and to map P' onto the outside one. Note that this collapses a neighborhood of ∂P as this simple closed curve lies on our sphere, which in turn is immersed into K', and thus eventually onto Y. This clears up the problem mentioned above. We record the images of P, P'.

$$P \to P + L + A + dr + dl; P' \to P' + L + L' + A + A' + O + O' + d;$$

where $d = dl + dr + dt + db$.

To see that g has a dense orbit, as well as its periodic points dense, it suffices to show that beginning with any cell, say C, of Y, consider the complete cells that g maps homeomorphically onto, throwing away any partial cells hit (even if several of these partial cells cover a whole cell). Then consider the whole cells that each of these cells hits under g, and so on. We need to show that in this manner, eventually all cells of Y are hit.

Here is the computation:

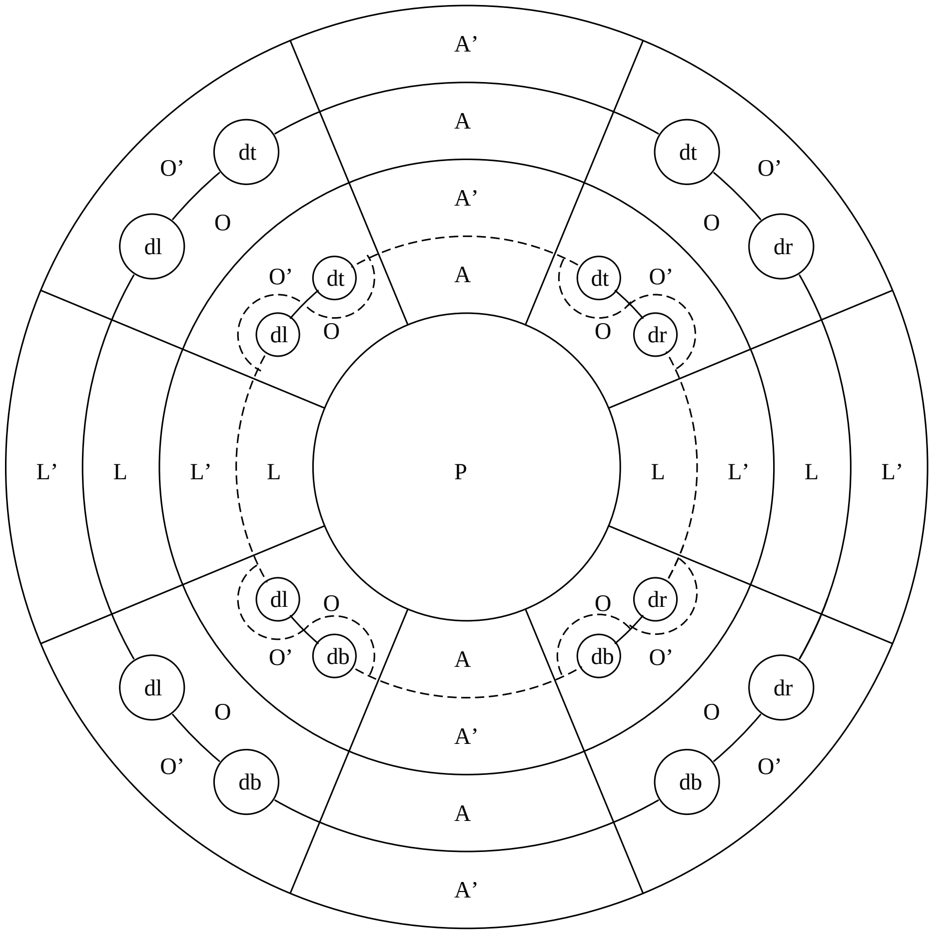

Figure 13

First note that the image of P' is all of Y except P and since A hits P this is all of Y, after 2 images. As the image of P contains dr, it second image contains L', so that its third image hits P' and hence eventually maps onto. As each of A, A', L, L' hits P or P' they eventually map onto. Finally, as each disk hits one of A, A', L, L', we are done.

6. Conclusion

Our example Y has 4 disks, 2 octagons an arm of 2 cells, a leg of 2 cells and 2 plates, a total of 12 cells. We were unable to reduce this number, keeping to disks as cells. In addition, we tried to keep the map as simple as possible. Our score:

1. each disk dx maps onto 3 cells and 4 partial cells: 12, 16.
2. each of O, O' maps to 11 cells and 8 partials: 22, 16

3. each of A, L maps to 1 cell and 4 partials: 2, 8.
4. each of A', L' maps to 5 cells and 8 partials: 10, 16.
5. P maps to 9 cells and 8 partials: 9, 8.
6. P' maps to 36 cells and 8 partials. 36, 8.
7. total 95 cells and 72 partials.

References

[AP] Jared Anderson and Ian Putnam, Topological invariants for substitution tilings and their associated C* algebras, Ergodic Theory and Dynamical Systems **18** part 3 (1998) 509–538.

[BLV] Marcy Barge, James Jacklitch, and Gioia Vago, Homeomorphisms of one-dimensional inverse limits with application to substitution tilings, unstable manifolds, and tent maps, Contemporary Mathematics, **246**, 1 - 15.

[FJ] F. T. Farrell and L. E. Jones, New attractors in hyperbolic dynamics, Journal of Differential Geometry **15**, no. 1 (1980), 107–133.

[M] Martin, George E., Polyominoes, The mathematical association of America,1991.

[MPP] Z. Masáková, J. Patera, E. Pelantová, Substitution rules for cut and project sequences, preprint.

[R] Robinson, Clark, *Dynamical Systems*, CRC Press,1995

[S] S. Smale, Differential dynamical Systems, Bulletin of the American Mathematical Society, 73 (1967) 746-817.

[T] W. Thurston, Groups, Tilings, and finite state automata, AMS colloquium lectures notes, Boulder, 1989.

[W1] R. F. Williams One dimensional nonwandering sets, Topology **6**,(1967), 473–487.

[W2] R. F. Williams, Expanding attractors, Institute des Hautes Études Scientifique Publ. Math. no. 43(1973), 169–203.

[W3] R. F. Williams, Spaces that won't say no. International conference on dynamical systems, Montevideo, Ledrappier, Lewowicz, and Newhouse, editors, Pitman Research notes in Mathematics number 362, Longman (1996) 236-46.

[W4] R. F. Williams, Higher dimensional continued fractions via geometric bifurcation, pre-preprint, University of Texas, Austin.

R.F. Williams
Department of Mathematics
The University of Texas at Austin
Austin, TX 78712 U.S.A.
bob@math.utexas.edu